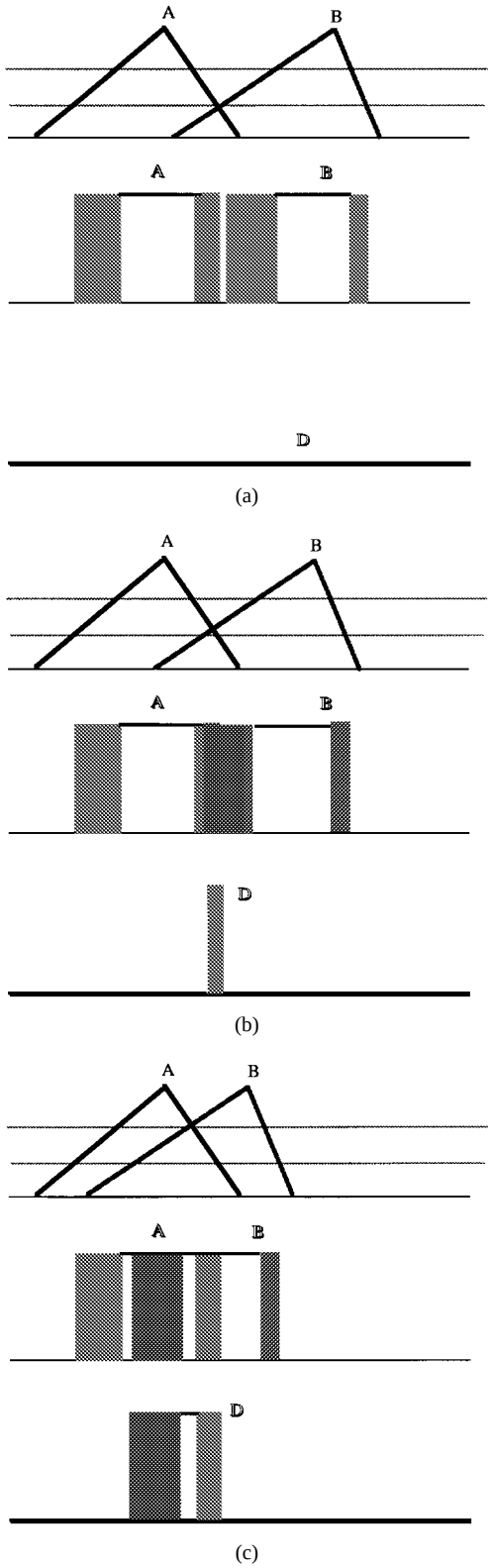

Fig. 17. Decision-making with shadowed sets; see description in text.

could be especially important in all situations where a certain trade-off between numeric precision and computational effort becomes necessary. Shadowed sets enhance and simplify an interpretation of results of processing with fuzzy sets by proposing decision expressed in the language of three-valued logic (that could be interpreted as yes, no, and unknown). As numeric details are suppressed while computing efficiency increased, one can think of shadowed sets as a provider of a quick and dirty approach to computing with fuzzy quantities—if the obtained results are of interest (usually shadowed sets with nonempty cores) then one can resort to detailed yet time consuming computing with fuzzy sets.

REFERENCES

[1] R. E. Bellman and L. A. Zadeh, "Decision making in a fuzzy environment," *Manage. Sci.*, vol. 17, pp. 141–164, 1970.
[2] J. C. Bezdek, *Pattern Recognition with Fuzzy Objective Functions*. New York: Plenum, 1981.
[3] K. Hirota, "Concepts of probabilistic sets," *Fuzzy Sets Syst.*, vol. 5, pp. 31–46, 1981.
[4] A. Kandel, *Fuzzy Techniques in Pattern Recognition*. New York: Wiley, 1982.
[5] G. J. Klir and T. A. Folger, *Fuzzy Sets, Uncertainty, and Information*. Englewood Cliffs, NJ: Prentice-Hall, 1988.
[6] M. Mizumoto and K. Tanaka, "Some properties of fuzzy sets of type 2," *Inf. Contr.*, vol. 31, pp. 312–340, 1976.
[7] Z. Pawlak, *Rough Sets*. Dordrecht, The Netherlands: Kluwer, 1991.
[8] T. Radecki, "Level fuzzy sets," *J. Cybern.*, vol. 7, pp. 189–198, 1977.
[9] N. Rescher, *Many-Valued Logic*. New York: McGraw-Hill, 1969.
[10] R. Sambuc, "Fonctions Φ-flous. Application a l'aide au diagnostic en pathologie thyroidienne," Ph. D. dissertation, University of Marseille, Marseille, France, 1975.

Fault-Tolerant Locomotion of the Hexapod Robot

Jung-Min Yang and Jong-Hwan Kim

***Abstract*—In this paper, we propose a scheme for fault detection and tolerance of the hexapod robot locomotion on even terrain. The fault stability margin is defined to represent potential stability which a gait can have in case a sudden fault event occurs to one leg. Based on this, the fault-tolerant quadruped periodic gaits of the hexapod walking over perfectly even terrain are derived. It is demonstrated that the derived quadruped gait is the optimal one the hexapod can have maintaining fault stability margin nonnegative and a geometric condition should be satisfied for the optimal locomotion. By this scheme, when one leg is in failure, the hexapod robot has the modified tripod gait to continue the optimal locomotion.**

I. INTRODUCTION

During the past decades, there have been many studies on multi-legged walking robots. It is generally recognized that natural legged systems have many advantages in the mobility characteristics over wheeled or tracked vehicles. This is attributed to their inherently greater adaptability to terrain irregularities and their superior off-road mobility in comparison to wheeled or tracked vehicles.

Terrain adaptive locomotion involves intelligent foothold selection and the control of gait to produce a desired motion. The terrain

Manuscript received March 18, 1995; revised November 7, 1995 and July 20, 1996.

The authors are with the Department of Electrical Engineering, Korea Advanced Institute of Science and Technology (KAIST), Taejon-shi 305-701, Korea (e-mail: johkim@vivaldi.kaist.ac.kr).

Publisher Item Identifier S 1083-4419(98)02183-9.

adaptivity of a walking machine has been studied from two distinct viewpoints. First, much of previous work has been devoted to the leg sequencing problems for periodic locomotion over level ground terrain. The standard periodic gait for straight line walking is the wave gait in which the locomotion is characterized by a forward wave of stepping actions on each side of the body with a half-cycle phase shift between the two sides. As early as 1960, McGhee and Frank [1] proved that a quadruped wave gait has the optimum stability among all quadruped periodic and regular gaits. Bessonov and Umnov [2] extended that result to the hexapod motion in straight lines. Recently, Song and Choi [3] reported the optimally stable ranges of generalized $2n$-legged wave gaits.

In reality, however, there may be terrains which are not even, such as soft soil, rocks, holes, etc. This triggered research on the terrain adaptivity from the second point of view: given a desired motion trace of the walking machine, how should one plan the lifting and placing of legs so as to avoid stepping over the rough terrain on the ground? The resulting gait has been termed the free gait to distinguish from the wave gait. The problem of generating a free gait was first recognized, formalized, and solved for a hexapod robot by Kugushev and Jaroshevskij [4], and subsequently improved upon by McGhee and Iswandhi [5]. Besides free gaits, follow-the-leader (FTL) gaits [6], adaptive gaits [7], and others have been proposed to overcome rough terrain.

In spite of many results from the two viewpoints, there has been little interest in coping with possible failure events effectively in the locomotion of multilegged robots. Fault tolerance is an essential factor in ensuring successful autonomous systems, especially robots working in remote or hazardous environments [8]. To avoid cost and risk involved in sending humans into these environments and improve the probability of mission success, robots must be able to quickly detect and tolerate internal or external failures without relying on immediate repairs or human intervention. In developing robotic fault detection and tolerance algorithms, the possible failures within the robot and the interdependence of these failures must firstly be determined. In multilegged robot systems, fault events may result from unexpected changes in walking machine's environment, or internal damages such as loss of sensor input and failure of the end effector of a leg. In [9], a distributed neural network controller for locomotion based on insect neurobiology has been used to control a hexapod robot and demonstrated to have robustness on several faults. In [10], two modes of stability, stance stability and walker stability, were defined and developed to take into account the effect of walker/terrain compliances and provide a tool for maintaining stability in the presence of disturbance according to walker configuration on the stability of the walker.

In this paper, we derive the fault-tolerant locomotion of the hexapod walking robot on even terrain. Several kinds of fault events that can occur during the locomotion of the hexapod robot are defined and efficient methods of fault detection are proposed. For fault-tolerant capability, we define *the fault stability margin* and prove that the hexapod can accommodate a fault event if its gait has a nonnegative fault stability margin. We derive the optimal fault-tolerant gait sequence for the straight line motion of the hexapod on even terrain. Also, the modified tripod gait sequence is defined and we prove that it is the optimal gait the hexapod can have when a fault event occurs in a leg.

II. Representation of the Hexapod Robot

A simplified two-dimensional model of a hexapod robot is shown in Fig. 1. C is the center of gravity of the machine and the origin of the machine coordinate system. Leg numbers of the hexapod are assigned as 1, 2, 3 on the left-hand side and 4, 5, 6 on the right-hand side, as shown in Fig. 1. In this paper, the following assumptions are made for the simplicity of analysis.

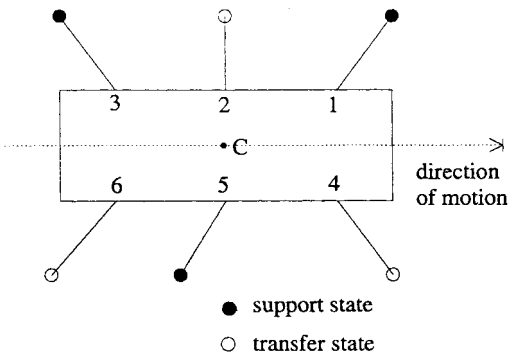

Fig. 1. Two-dimensional model of a hexapod robot.

1) The hexapod has a symmetric structure.
2) The contact between a foot and the ground is a point.
3) There is no slipping between the foot and the ground.
4) All the mass of the legs is lumped into the body, and the center of gravity is assumed to be at the centroid of the body.
5) The initial foothold positions should be at the specified locations before the locomotion starts.
6) Unless specified otherwise, the speed of the hexapod body when it moves and the average speed of each leg during the transfer phase are constant.

In the multilegged robot system, the state of a leg is either support or transfer. Thus if we assign the number 1 to the *support state* and 0 to the *transfer state*, the whole states of six legs at any time can be represented by a 1×6 vector $\mathbf{q}$ such that

$$\mathbf{q} = (q_1, q_2, q_3, q_4, q_5, q_6), \quad q_i \in \{1, 0\} \tag{1}$$

where q_i indicates the state of leg i.

By definition, an event of a gait is the placing or lifting of a leg during locomotion. We define the set of events as

$$E = \{u_i, d_i \colon i = 1, 2, \ldots, 6\} \tag{2}$$

where d_i is the event of the placing of the leg i and u_i is the event of the lifting of the leg i. Here d means a "down" motion and u means an "up" motion of each leg.

States of legs are changed by these events. The state transition of leg i is described as follows:

$$\begin{aligned} q_i \colon 1 &\xrightarrow{u_i} 0 \\ q_i \colon 0 &\xrightarrow{d_i} 1. \end{aligned} \tag{3}$$

The transition of the overall leg states $\mathbf{q}$ will be expressed similarly.

Each leg has a reachable area in the form of a sector of an annulus. Since overlapping reachable areas raise interference problems, one way to solve it is to eliminate *a priori* all the overlapping reachable areas altogether so that each leg has a distinct region which can be accessed only by itself and not by any other leg. In this paper, we redefine a rectangular region as *a reachable cell* of each leg as shown in Fig. 2.

III. Fault Detection

There are many kinds of failure events in the dynamics of the hexapod robot. They may stem from unexpected changes in outer environment such as tracing into rough or uneven terrain or internal failures within the robot system. Several kinds of fault cases are: a failure of robot sensor input, a loss of a leg's end effector, a failure

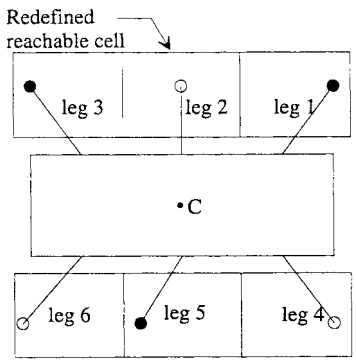

Fig. 2. Redefined reachable cell of each leg.

of communication between controller and end effectors, a failure of controller itself, and delays in response to commanded position changes. In this paper, we consider the following two failures:

1) failure in the kinematic part of a leg;
2) failure of communication between controller and a leg effector.

1) is a fault event in which a lift motor for a leg or a kinematic part of a leg breaks down so that the leg cannot maintain its *support state*, i.e., support the robot's weight. 2) is a fault event that the channel between controller and a leg effector is disabled. If 2) occurs on one leg, the leg cannot change its state and must remain its present position and state until completely recovered. Let "b_i" denote the event that fault 1) occurs to leg i and "c_i" the event that fault 2) occurs to leg i.

The above faults can be detected by watching changes of the leg state $\mathbf{q}$ and the success or failure of firings of normal events. First, let us consider the occurrence of b_i. If the present state of leg i is *support*, then b_i causes the state of leg i to transfer state even though the lifting event u_i is not fired. So the occurrence of b_i can be detected when leg i is transformed to transfer state *without* firing of u_i. That is, the following transition can be regarded as a fault b_i:

$$q_i\colon 1 \xrightarrow{b_i} 0 \quad \text{without } u_i. \tag{4}$$

However, if the present state of leg i is *transfer*, the occurrence of b_i cannot be caught until the placing event d_i is fired. We can become aware of the occurrence of b_i only when the firing of d_i can't make leg i be in support state. Thus we get the following result:

$$q_i\colon 0 \xrightarrow{d_i} 0 \quad \text{after } b_i \text{ occurs.} \tag{5}$$

The occurrence of c_i is similar to the case of b_i when $q_i = 0$. Even though the state of leg i is not changed immediately at the time c_i happens, we can see the following fault occurrences when an event d_i or u_i cannot take the proper operation any more:

$$\begin{aligned} q_i\colon 0 &\xrightarrow{d_i} 0 \\ q_i\colon 1 &\xrightarrow{u_i} 1. \end{aligned} \tag{6}$$

From the analysis above, we can define the following fault detection profile.

Fault Detection Profile: Occurrence of a fault event in the dynamics of the hexapod robot is detected when a normal state transition of a leg or a proper firing of a normal event fails to function in a desired manner.

IV. Fault Tolerant Locomotion

A. Problem Statements

With the fault detection profile established, we propose in this section fault-tolerant control of the hexapod robot locomotion on even terrain. For the clarity of presentations of concepts, we specify fault occurrence situations by assuming the following:

i) The hexapod robot moves along the straight line on even terrain.
ii) Only one fault event occurs during a whole locomotion.
iii) The fault is not recovered during the locomotion.

In our discussion, we exclude the case where c_i occurs at $q_i = 1$. It is the only case that causes leg i to be in support state after fault occurrence. So if not recovered during the locomotion as was assumed, the hexapod should manage to drag the leg, which is a very abnormal situation. To treat with such a defect will be another problem. Thus we focus on developing schemes to tolerate fault events which prevent one leg from maintaining support state.

B. Quadruped Gait

We assume that in even terrain locomotion the hexapod is moving in the $+X$-axis direction. Based on the previous assumptions and the definition of stability margin [5], we define the *fault stability margin*.

Definition 1: Fault stability margin S_f of a gait is the minimum of stability margins of gaits generated by changing alternately the state of one supporting leg of the gait to transfer state and maintaining the other legs' states.

The fault stability margin defined above has the same meaning of the stability margin of the *conservative support polygon* (CSP) proposed by Nagy *et al*. [10], which was defined to be the intersection of n support patterns made by all the combinations of $n-1$ supporting legs where n is the number of legs of the multilegged robot. It is clear $S_f < S_m$ for any gait where S_m is the stability margin of the gait. S_f means the degree of potential stability to which the hexapod is guaranteed its stability in case one of the supporting legs becomes transfer state abruptly *by fault occurrence*. In calculating the fault stability margin, it is not necessary to consider the transfer legs because the stability margin of a gait is derived only by the positions of supporting legs and the states of transfer legs do not change after occurrence of a fault event b_i or c_i. With the notion of fault stability margin defined, we have the following theorem which is fundamental to the fault-tolerant locomotion.

Theorem 1: For the hexapod robot to be stable without regard to fault occurrence, the gait must have $S_f \geq 0$ during a whole locomotion.

This theorem is valid even in rough terrain locomotion. To secure a nonnegative fault stability margin, the hexapod should not have any tripod gait at all because $S_f < 0$ for all tripod gaits. Thus for the optimal straight line locomotion, we must investigate the existence of periodic quadruped gaits guaranteeing $S_f \geq 0$.

Fig. 3 shows the redefined reachable cells and the robot body with specific foothold positions. P and Q denote the size of a cell, W is the distance between the reachable cell and the robot body, and U is the width of the robot body. For the robot, we postulate the following theorem.

Theorem 2: Let the initial foothold of each leg be the middle foothold position as in Fig. 4(a). Then the sequence of optimal quadruped gait locomotion guaranteeing nonnegative fault stability margin is that in Figs. 4 and 5.

Proof: At the initial position, all the possible combinations of two legs which can be lifted maintaining nonnegative fault stability margin are (leg 1, leg 6), (leg 2, leg 5), and (leg 3, leg 4). Of them, by symmetry of the geometry of the hexapod, the choice of (leg 1, leg 6) will yield the same result as that of (leg 3, leg 4), so we should choose either (leg 3, leg 4) or (leg 2, leg 5) as the initially lifted legs. We select lifting of leg 3 and leg 4 because it has a less restrictive constraint than the lifting of leg 2 and leg 5, which will be analytically

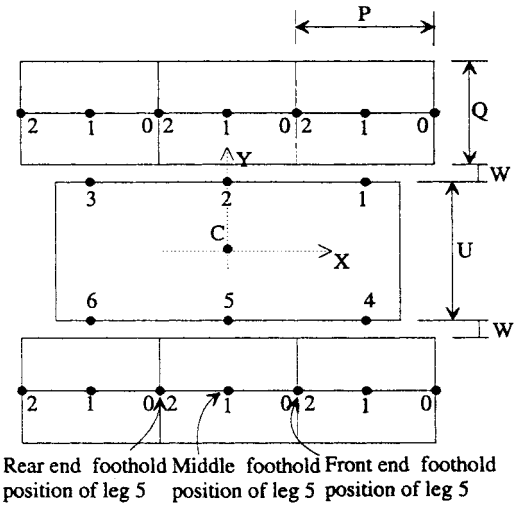

Fig. 3. The scale of reachable cells and the robot body.

proved later. The maximum stride length the two lifted legs may have is $\frac{1}{2}P$, or half the pitch as Fig. 4(c) because their initial footholds are the middle foothold positions in Fig. 3. For lifting leg 2 and leg 5 at Fig. 4(c) without reducing S_f to negative, the center of gravity must move to point A in Fig. 4(d). After placing leg 2 and leg 5 at the front end foothold positions like Fig. 4(f), we again move the center of gravity to B in Fig. 4(g) to lift leg 1 and leg 6 guaranteeing marginal fault stability margin. Finally, with leg 1 and leg 6 placed at front end foothold positions, the hexapod goes through one complete locomotion cycle. It is sure during the cycle all the legs have the optimal stride lengths with $S_f \geq 0$. □

As the position of the center of gravity changes, all the six reachable cells must move accordingly because the position of each reachable cell depends on that of the center of gravity. But in Fig. 4 we temporarily fixed the positions of reachable cells at the initial points. It is for the purpose of more effectively illustrating the stride length of lifting legs and the lapse of the period of the quadruped gait sequence. The minimum longitudinal stability margin during a cycle is $\frac{1}{2}P$ [see Fig. 4(b) and (h)].

It should be noted that in the above sequence the body of the hexapod moves not only in the $+X$-axis direction but also in the $\pm Y$-axis direction as in Fig. 4(d) and (g). However, because all the legs remain support states in the movement of the center of gravity, a geometric constraint about redefined reachable cells must be satisfied.

Theorem 3: Fig. 6 is the support pattern of Fig. 4(d) with scales defined in Fig. 3. Then, for the center of gravity to move to point A, the following condition must be satisfied:

$$Q \geq \frac{1}{3}(U + 2W). \tag{7}$$

Proof: By some mathematical manipulations, m is expressed as

$$m = \frac{1}{8}(Q + U + 2W). \tag{8}$$

As the center of gravity moves m in the $+Y$-axis, the position of the redefined reachable cell transfers the same distance. But the foothold position of each leg does not change. So for all the foothold positions of legs to be within the shifted reachable cells, the following inequality must be valid:

$$\frac{Q}{2} \geq m. \tag{9}$$

From (8) and (9),

$$Q \geq \frac{1}{3}(U + 2W). \qquad \square$$

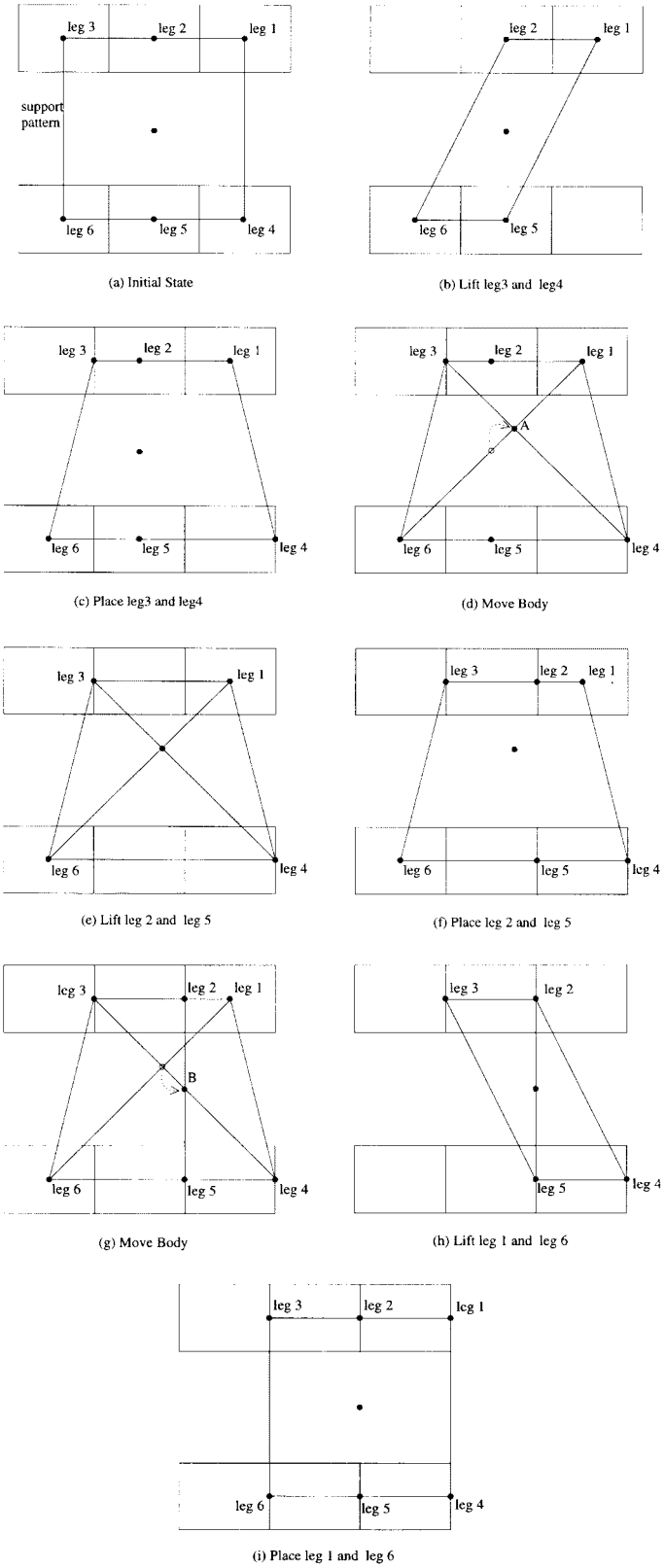

Fig. 4. The quadruped gait with nonnegative fault stability margin in a locomotion cycle.

Inequality (7) is the necessary condition to enable a fault-tolerant quadruped gait on even terrain when the shape of redefined reachable cells is rectangular. We should take into account this condition in real design of the hexapod robot to guarantee the optimal fault-tolerant quadruped gait.

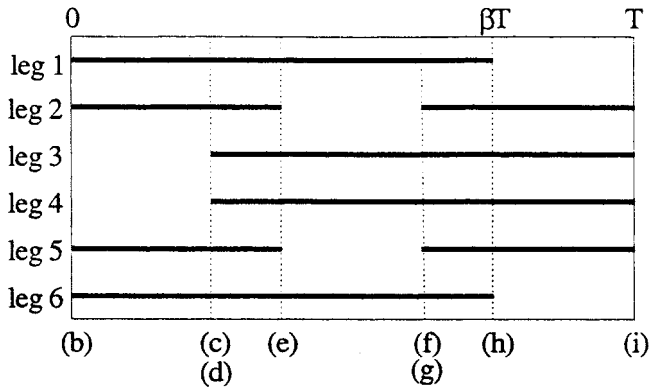

Fig. 5. Time diagram of the quadruped gait in Fig. 4. The solid line indicates support phase.

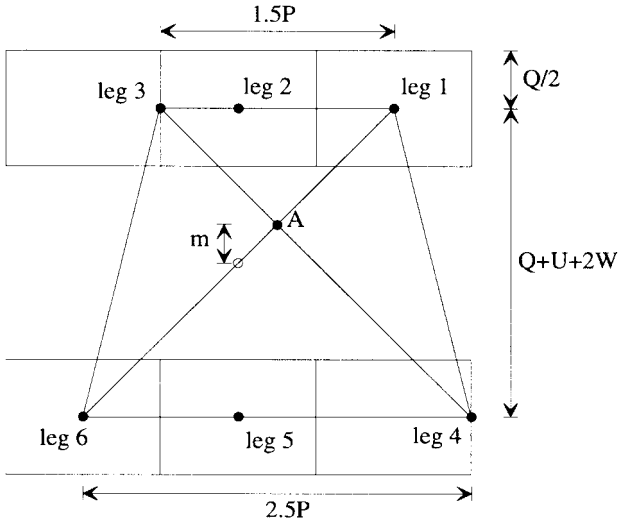

Fig. 6. Geometric condition of the quadruped gait.

Now we explain the reason why the combination of leg 2 and leg 5 cannot be a candidate for the initially lifted legs in Theorem 2. If leg 2 and leg 5 had moved the maximum stride length to the front end foothold positions, the next lifted legs must be (leg 1, leg 6) or (leg 3, leg 4) for the optimal locomotion. If we choose leg 1 and leg 6, then the center of gravity must move to A as in Fig. 7. Then m, the moving distance of the center of gravity in the $-Y$-axis direction, is easily computed as follows:

$$m = \frac{1}{4}(Q + U + 2W). \tag{10}$$

Therefore, from (9) and (10), the geometric condition for the foothold position to be in the shifted reachable cell is

$$Q \geq U + 2W. \tag{11}$$

Comparing (11) with (7), we can find out that (11) is more restrictive because the width of a reachable cell Q must be three times wider than that of (7) if the other scales are the same. So the gait sequence in Fig. 4 is a more general sequence of fault-tolerant quadruped gait.

Let v_l be the average speed of leg swing and v_b the speed of robot body movement in the $+X$-axis. From Fig. 4, the stride length of each leg is $\frac{1}{2}P$ and the total distance that the body moves in a locomotion cycle is $\frac{1}{2}P$. Hence the period T and duty factor β, which is defined to be the time fraction of a cycle in which a leg is in the support state [5], can be derived from Fig. 5 as

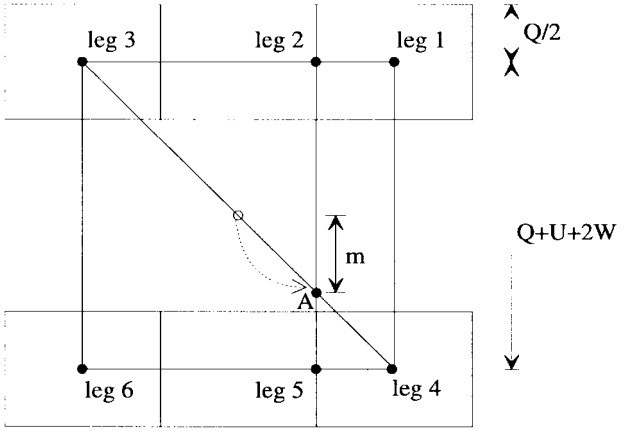

Fig. 7. Gait form after leg 2 and leg 5 were initially lifted.

$$T = 3\frac{\frac{1}{2}P}{v_l} + \frac{\frac{1}{2}P}{v_b} \tag{12}$$

$$\beta = \frac{2\frac{\frac{1}{2}P}{v_l} + \frac{\frac{1}{2}P}{v_b}}{3\frac{\frac{1}{2}P}{v_l} + \frac{\frac{1}{2}P}{v_b}} = \frac{v_l + 2v_b}{v_l + 3v_b}. \tag{13}$$

For the comparison of the stability margin with the conventional wave gait, we assume that the average speed of leg swing equals the speed of robot body movement, or $v_l = v_b$. Then β is $\frac{3}{4}$ and, by Lemma 5 of [3], the longitudinal stability margin of the wave gait of the hexapod is $\frac{1}{2}P$, equal to the value of the fault-tolerant quadruped gait. Therefore it can be said that the fault-tolerant quadruped gait derived in Theorem 2 maintains the stability margin with respect to the wave gait.

In the gait of Figs. 4 and 5, we set the stride length of each leg half the pitch for the optimality of the gait. But our gait will be generalized to have other stride lengths. Fig. 8 shows the case of stride length R $(<\frac{1}{2}P)$. Theorem 3 will be adapted accordingly.

C. Tripod Gait

Since it was assumed that only one fault event occurs during a whole locomotion, once a fault has occurred to a leg we don't need to consider S_f any more. Therefore the hexapod can have tripod gait for optimal locomotion after fault occurrence. We derive the hexapod tripod gaits with one leg in failure. The proposed sequences are similar to the sequence developed by Lee *et al*. [11]. But in our case, only five legs may function well so that the sequence of lifting and placing of legs is different from the conventional tripod gait. We derive the sequences for two situations where a fault occurs to leg 1 and leg 2, respectively, in the locomotion. By geometric symmetry of the hexapod, the sequence for leg 3, 4, or 6 in failure is very similar to that of leg 1 failure case and the sequence for the case of leg 5 is very similar to that of leg 2.

Theorem 4: Let the initial foothold of each leg be as in Fig. 9(a) when a fault occurs to leg 1. Then the sequence of optimal tripod gait locomotion with zero longitudinal stability margin is that in Figs. 9 and 10.

The proof is very similar to that of Theorem 2. The gait sequence has zero longitudinal stability margin and zero kinematic limit margin [5]. The sequence can be extended to generate gaits with nonzero longitudinal stability margins as in [11].

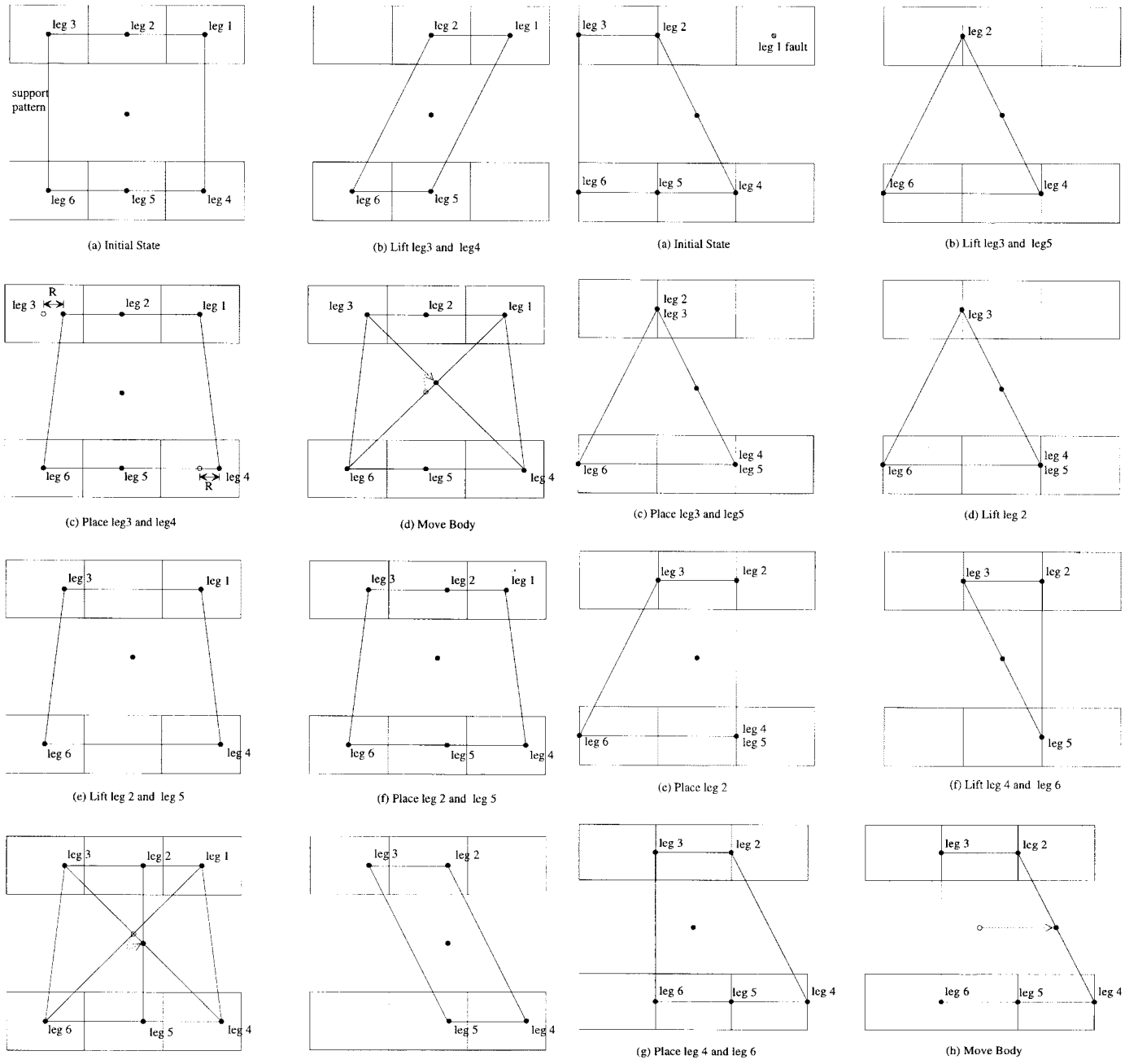

Fig. 8. The quadruped gait with nonnegative fault stability margin in a locomotion cycle and the stride length R ($<\frac{1}{2}P$).

Fig. 9. The tripod gait with leg 1 in failure.

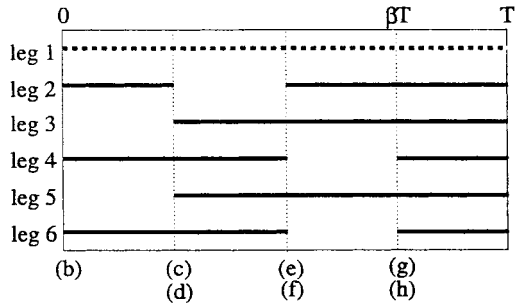

Fig. 10. Time diagram of the tripod gait in Fig. 9. The solid line indicates support phase.

Although we assumed the initial state of the tripod gait with leg 1 in fault is Fig. 9(a), it should be noted that even if a fault occurs to leg 1 at any state among (a)∼(i) in Fig. 4 during a locomotion cycle, the state can be switched to one of (a)∼(h) in Fig. 9 by simply changing the position of supporting legs or the center of gravity.

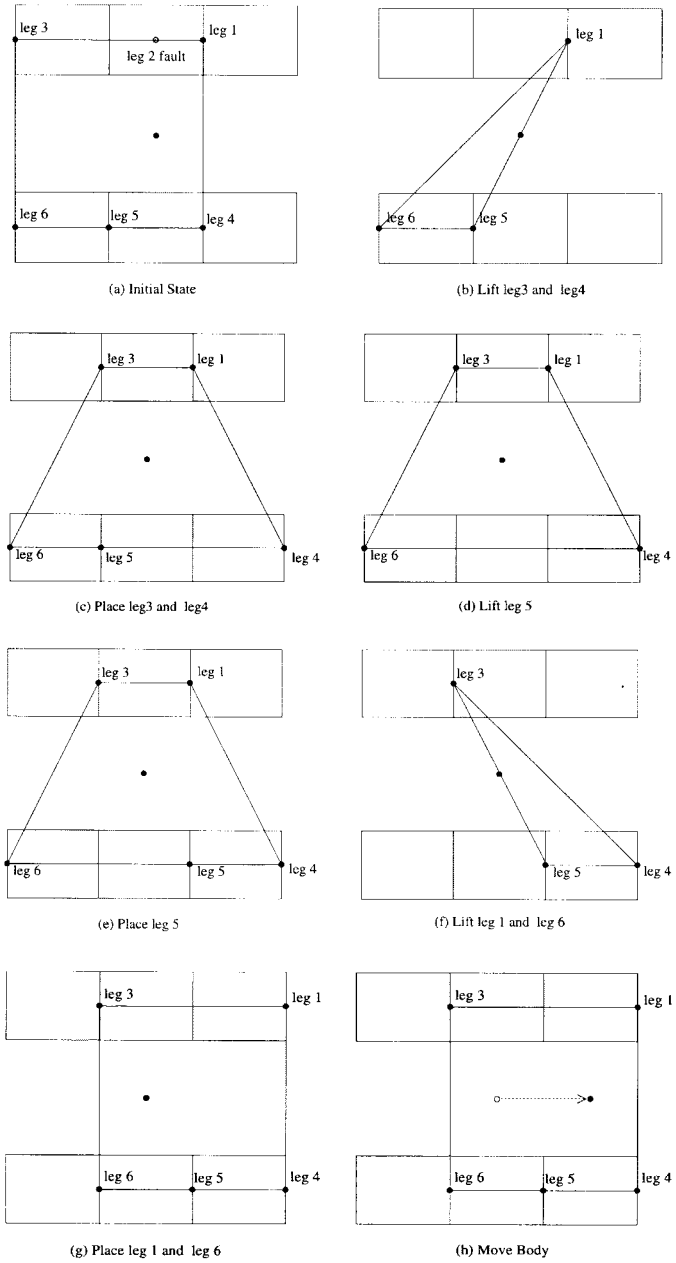

Fig. 11. The tripod gait with leg 2 in failure.

The period and duty factor can be similarly calculated as in the quadruped gait. From Fig. 10

$$T = 3\frac{P}{v_l} + \frac{P}{v_b} \tag{14}$$

$$\beta = \frac{2\frac{P}{v_l} + \frac{P}{v_b}}{3\frac{P}{v_l} + \frac{P}{v_b}} = \frac{v_l + 2v_b}{v_l + 3v_b}. \tag{15}$$

Duty factor derived above is identical to the result of the quadruped gait. But each leg's stride length and the distance the center of gravity moves are twice those of the quadruped gait. So the tripod gait has twice the period of the quadruped gait.

Figs. 11 and 12 show the sequence of the tripod gait after a fault occurs to leg 2. The analysis of the gait sequence can be done in the same way.

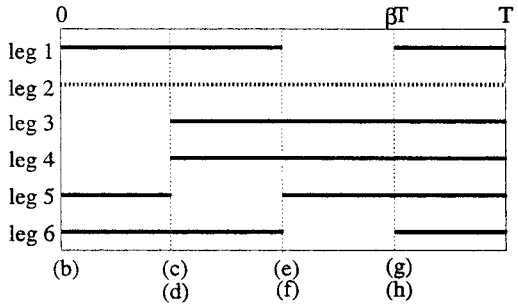

Fig. 12. Time diagram of the tripod gait in Fig. 11. The solid line indicates support phase.

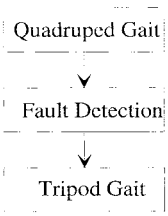

Fig. 13. Block diagram of the fault-tolerant locomotion of the hexapod.

Fig. 13 is the overall block diagram of the fault-tolerant locomotion of the hexapod robot on even terrain. As shown in the figure, the hexapod has the quadruped gaits of Fig. 4 in a normal state. When a fault is detected by the fault detection process described in the previous section, the hexapod robot changes its gait to the tripod gait sequence which is illustrated in Figs. 9 and 11. As was analyzed, the duty factor maintains the same value and the period increases twice when the hexapod changes its gait from the quadruped to the tripod. But the distance the center of gravity moves in a period also grows twice. Thus, the resulting speed of the gait remains the same without regard to a fault occurrence.

The longitudinal stability margin is reduced from $\frac{1}{2}P$ [Fig. 4(b) and (h)] to zero when the hexapod gait changes mode to tripod by a fault occurrence. But the hexapod could have a nonzero longitudinal stability margin by slightly changing the sequences of Fig. 9 and 11 at the cost of increase of the duty factor and decrease of the stride length of leg, and hence, degradation of optimality.

V. Conclusion

In this paper, the fault-tolerant locomotion of the hexapod robot on even terrain was proposed. Several fault events that can happen to the multilegged walking machine were defined and effective detection methods were proposed. The fault stability margin was defined to represent potential stability a gait can have in case of a sudden fault event to one leg. Based on this, the fault-tolerant quadruped periodic gaits of the hexapod walking over perfectly even terrain was derived. It was demonstrated that the quadruped gait derived in this paper is the optimal one the hexapod can have maintaining fault stability margin nonnegative. When a fault occurs to a leg, the hexapod changes its gait to the tripod gait. But in this case, only five legs function well so that the sequence of lifting and placing of legs is different from the conventional tripod gait. We proposed the tripod gait sequence that has zero longitudinal stability margin and zero kinematic limit margin. General fault-tolerant gaits having nonzero longitudinal stability margins and kinematic limit margins could be derived similarly by analogy.

REFERENCES

[1] R. B. McGhee and A. Frank, "On the stability of quadruped creeping gait," *Math. Biosci.*, vol. 3, no. 314, pp. 331–351, Oct. 1968.

[2] A. Bessonov and A. Umnov, "The analysis of gaits in six-legged vehicle according to their static stability," in *Proc. Symp. Theory Practice Robots*, Udine, Italy, 1973, pp. 1–9.

[3] S. M. Song and B. S. Choi, "The optimally stable ranges of $2n$-legged wave gaits," *IEEE Trans. Syst., Man, Cybern.*, vol. 20, July/Aug. 1990.

[4] E. I. Kugushev and V. S. Jaroshevskij, "Problems of selecting a gait for an integrated locomotion robot," in *Proc. 4th Int. Conf. Artificial Intelligence*, Tbilisi, U.S.S.R., Sept. 1975, pp. 789–793.

[5] R. B. McGhee and G. I. Iswandhi, "Adaptive locomotion of a multilegged robot over rough terrain," *IEEE Trans. Syst., Man, Cybern.*, vol. SMC-9, Apr. 1979.

[6] F. Ozguner, S. I. Tsai, and R. B. McGhee, "An approach to the use of terrain-preview information in rough-terrain locomotion by a hexapod walking machine," *Int. J. Robot. Res.*, vol. 3, pp. 134–146, Summer 1984.

[7] S. Hirose, "A study of design and control of a quadruped walking vehicle," *Int. J. Robot. Res.*, vol. 3, pp. 113–133, Summer 1984.

[8] M. Jamshidi and P. J. Eicker, *Robotics and Remote Systems for Hazardous Environments*. Englewood Cliffs, NJ: Prentice-Hall, 1993.

[9] H. J. Chiel, R. D. Beer, R. D. Quinn, and K. S. Espenshied, "Robustness of a distributed neural network controller for locomotion in a hexapod robot," *IEEE Trans. Robot. Automat.*, vol. 8, pp. 293–303, June 1992.

[10] P. V. Nagy, S. Desa, and W. L. Whittaker, "Energy based stability measures for reliable locomotion of statically stable walkers: Theory and application," *Int. J. Robot. Res.*, vol. 13, no. 3, pp. 272–287, 1994.

[11] T. T. Lee, C. M. Liao, and T. K. Chen, "On the stability properties of hexapod tripod gait," *IEEE J. Robot. Automat.*, vol. 4, pp. 427–434, Aug. 1988.

Intelligent Compliant Motion Control

Omar M. Al-Jarrah and Yuan F. Zheng

***Abstract*—The role of a compliant motion scheme is to control a robot manipulator in contact with its environment. By accommodating with the interaction force, the manipulator can be used to accomplish tasks that involve constrained motions. This paper presents a new work on the compliant motion control for position-controlled manipulator. A new method for achieving efficient interaction between the manipulator and its environment is developed. The interaction force is reduced using a quadratic cost function. In this method, the compliance is formulated as function of the interaction force. An adaptive element is used to update the compliance. The stability of the system is investigated using the Lyapunov approach. Experiments are conducted in our laboratory to demonstrate the use of such scheme.**

I. INTRODUCTION

Many applications in the manufacturing and service industries require manipulators to make contact with environments [1]–[4]. For example, inserting a peg in a hole, turning a crank, grinding, polishing, teleoperating, and bending a flexible beam. Its common to all of those applications that the motion of the manipulator's end-effector is constrained by the environment. In recent years, two notable approaches dealing with this problem have been proposed. One approach uses a hybrid position/force control scheme to control the position in those directions where there is no constraint and to control the force in the constrained direction [5], [6]. The second approach realizes the fact that the end-effector must comply with the interaction force. Otherwise, rejecting the interaction force will result in instability and possibly damage to either the end-effector or the environment or both. This can be done using a compliant motion control scheme [7].

Compliance can be either passive or active. Passive compliance is achieved by attaching a spring-damper device to the end-effector. Remote center compliance (RCC) is an example of passive compliance which is used for the peg-in-a hole problem [8]. Passive devices such as RCC are task-oriented devices and places extra loading on the end-effector. On the other hand, active compliance uses a compliant motion control scheme which is not restricted to a specific task and places no loading on the end-effector.

The core of the active compliant motion is the concept of mechanical impedance in which both the dynamic behavior and the position of the manipulator are controlled [9]. Several adaptive compliant and impedance motion control schemes were devised [7], [10]–[13]. It is common for those schemes to use combinations of proportional, integral, and derivative controls plus nonlinear compensation for the gravity, centrifugal, and coriolis terms in the manipulator dynamics.

Compliant motion introduces a force feedback loop which affects the stability of the system. Stability analysis of several compliant control schemes has been addressed by several researchers. The stability of the system depends on the desired impedance parameters. The impedance of the environment greatly affects the stability analysis of the system.

In a position control system, compliant motion is similar to what is believed to take place in biological systems [14]. Control of human movement is believed to have a hierarchical structure of three levels. The highest level in the motor control hierarchy is in the association cortex in which needs are converted into motor plans that are relevant to the context. The middle level is the projection system in which motor plans are transformed into motor programs that control different aspects of motion. Motor programs are updated according to the tasks (learning). The spinal cord is the lowest level in the motor control hierarchy. It converts the motor commands into muscular activity which are regulated by the spinal cord using reflexes.

In this paper, a new compliant motion control scheme is proposed based on what is believed to take place in biological systems. In this scheme, the compliance of the manipulator is changed in accordance with the sensed force and varies in a way that speeds up the reduction of the interaction forces. To accomplish this, a quadratic cost function is defined on the interaction force and the compliance is updated in the steepest decent direction. The stability of the proposed scheme is investigated using the Lyapunov approach.

This paper is organized as follows. Intelligent compliant motion control is formulated in the next section. The third section is devoted for studying the stability of the system. Advantages and limitations of this approach are discussed in the fourth section, while the fifth section presents an application for this scheme. The experimental results are presented in the sixth section. Finally, the paper is concluded in the seventh section.

II. INTELLIGENT COMPLIANT MOTION CONTROL

We will consider the case where the compliance is provided for the robot using an external control loop as shown in Fig. 1. Consider

Manuscript received April 15, 1996; revised November 25, 1996. This work was supported by the National Science Foundation under Grant IRI-9405276.

The authors are with the Department of Electrical Engineering, The Ohio State University, Columbus, OH 43210 USA (e-mail: zheng@ee.eng.ohio-stat.edu).

Publisher Item Identifier S 1083-4419(98)00215-5.